Published in final edited form as:
*Diabetes*. 2005 June ; 54(6): 1706–1716.

# The Link Between Nutritional Status and Insulin Sensitivity Is Dependent on the Adipocyte-Specific Peroxisome Proliferator–Activated Receptor-γ2 Isoform

**Gema Medina-Gomez**[1], **Sam Virtue**[1], **Christopher Lelliott**[1], **Romina Boiani**[2], **Mark Campbell**[1], **Constantinos Christodoulides**[1], **Christophe Perrin**[3], **Mercedes Jimenez-Linan**[1], **Margaret Blount**[1], **John Dixon**[4], **Dirk Zahn**[4], **Rosemary R. Thresher**[4], **Sam Aparicio**[4], **Mark Carlton**[4], **William H. Colledge**[1], **Mikko I. Kettunen**[5], **Tuulikki Seppänen-Laakso**[6], **Jaswinder K. Sethi**[1], **Stephen O'Rahilly**[1], **Kevin Brindle**[5], **Saverio Cinti**[2], **Matej Orešič**[6], **Remy Burcelin**[3], and **Antonio Vidal-Puig**[1]

[1]Department of Clinical Biochemistry, Histopathology, Physiology and Oncology, University of Cambridge/Addenbrooke's Hospital, Cambridge, U.K. [2]Institute of Normal Human Morphology, Faculty of Medicine, Ancona University, Ancona, Italy [3]Centre National de la Recherche Scientifique-UMR 5018, Paul Sabatier University, Toulouse, France [4]Paradigm Therapeutics, Cambridge, U.K. [5]Department of Biochemistry, University of Cambridge, Cambridge, U.K. [6]VTT: Technical Research Centre of Finland, VTT Biotechnology, Espoo, Finland.

## Abstract

The nuclear receptor peroxisome proliferator–activated receptor-γ (PPARγ) is critically required for adipogenesis. PPARγ exists as two isoforms, γ1 and γ2. PPARγ2 is the more potent adipogenic isoform in vitro and is normally restricted to adipose tissues, where it is regulated more by nutritional state than PPARγ1. To elucidate the relevance of the PPARγ2 in vivo, we generated a mouse model in which the PPARγ2 isoform was specifically disrupted. Despite similar weight, body composition, food intake, energy expenditure, and adipose tissue morphology, male mice lacking the γ2 isoform were more insulin resistant than wild-type animals when fed a regular diet. These results indicate that insulin resistance associated with ablation of PPARγ2 is not the result of lipodystrophy and suggests a specific role for PPARγ2 in maintaining insulin sensitivity independently of its effects on adipogenesis. Furthermore, PPARγ2 knockout mice fed a high-fat diet did not become more insulin resistant than those on a normal diet, despite a marked increase in their mean adipocyte cell size. These findings suggest that PPARγ2 is required for the maintenance of normal insulin sensitivity in mice but also raises the intriguing notion that PPARγ2 may be necessary for the adverse effects of a high-fat diet on carbohydrate metabolism.



Address correspondence and reprint requests to Antonio Vidal-Puig, Department of Clinical Biochemistry, University of Cambridge/ Addenbrooke's Hospital, Hills Road, Cambridge CB2 2QR, U.K. ajv22@cam.ac.uk.

Additional information for this article can be found in an online appendix at http://diabetes.diabetesjournals.org.


Europe PMC Funders Author Manuscripts

Peroxisome proliferator–activated receptor-γ (PPARγ) plays a central role in adipogenesis and insulin sensitivity. PPARγ is expressed as two isoforms, PPARγ1 and PPARγ2, which differ only in that PPARγ2 has 30 extra amino acids at its $NH_2$ terminus. Under physiological conditions, PPARγ2 is expressed almost exclusively in white and brown adipocytes, whereas PPARγ1 is also expressed in colon, macrophages, skeletal muscle, and liver (1). Although there is limited information regarding the functional differences between these two splice variants, PPARγ2 may be more adipogenic than PPARγ1 (2,3). PPARγ2 may play a distinct role in regulating insulin sensitivity as suggested by the strong epidemiological evidence that the PPARγ2-specific Pro12Ala variant influences diabetes susceptibility in humans (4).

We have shown that expression of PPARγ isoforms is differentially regulated by nutritional factors (5). Murine studies showed that PPARγ2 mRNA is markedly downregulated in white adipose tissue (WAT) by fasting and normalized by re-feeding (1). Similarly, PPARγ2 gene expression is increased in WAT by a high-fat diet (HFD) as well as in mouse models of diet-induced obesity (5). Studies using genetically modified mouse models have addressed the role of PPARγ in vivo (6). A proadipogenic role for PPARγ in vivo was supported by the global PPARγ-deficient and the hypomorphic PPARγ mouse models (7–9). In addition to a role in promoting adipogenesis, activation of PPARγ also improves insulin sensitivity (10). However, the characterization of the heterozygous PPARγ knockout mouse provided the paradoxical finding that mice with a 50% reduction in PPARγ gene dosage were resistant to HFD-induced obesity and were more insulin sensitive (11,12). Thus, a 50% decrease in PPARγ gene dose at the expense of both isoforms, γ1 and γ2, promoted a similar insulin-sensitizing effect as activating the receptor with a PPARγ-specific agonist.

To further understand PPARγ function in vivo, tissue-specific deletions of both PPARγ isoforms have been generated (9,13–15). In particular, adipose tissue–specific deletion of PPARγ results in congenital and progressive lipodystrophy associated with lipotoxicity and insulin resistance (9,13). PPARγ also plays a permissive role for fat deposition in peripheral organs, as indicated by the liver-specific PPARγ knockout mouse. However, in all of these tissue-specific mouse models, both PPARγ1 and PPARγ2 transcripts were inactivated. Recently, Zhang et al. (16) reported that selective disruption of murine PPARγ2 also produces lipodystrophic changes. Preliminary metabolic evaluation of those animals showed that they were insulin resistant. However, because animals with impaired adipose tissue differentiation become insulin resistant whatever the underlying etiology, it is unclear whether the insulin resistance observed in those mice is secondary to the lipodystrophy or more directly related to independent effects of PPARγ2 on insulin sensitivity. We have been able to address this question more directly by generating a mouse model of selective PPARγ2 deficiency, which develops morphologically normal adipose tissue. In these mice, we have performed detailed metabolic evaluations on both normal and HFDs, and we provide evidence that the PPARγ2 isoform is a critical link between nutritional state and insulin sensitivity.

## RESEARCH DESIGN AND METHODS

### Cloning of mouse PPARγ2 gene and targeting construct

A genomic mouse PPARγ2 clone was obtained from a 129-mouse strain P1 artificial chromosome genomic library (RPCI mouse P1 artificial chromosome library 21) to assemble a replacement targeting construct in which the PPARγ2-specific exon B1 was replaced with a IRESβGalMCNeo cassette, which contains LacZ/Neo cassette and HSVtk genes for positive and negative selection, respectively (online appendix [available at http://diabetes.diabetesjournals.org]).

### Animal care

Animals were housed four per cage in a temperature-controlled room (24°C) with a 12-h light/dark cycle. Food and water were available ad libitum unless noted. All animal protocols used in this study were approved by the U.K. Home Office.

### HFD studies and blood biochemistry

Wild-type and PPARγ2 knockout mice were placed at weaning (3 weeks of age) on either an HFD (45% calories from fat; D12492, Research Diets) for 28 weeks or a normal diet (10% calories from fat; D12450B, Research Diets). Enzymatic assay kits were used for determination of plasma free fatty acids (Roche), glycerol (Analox Instruments), and total triglycerides (Sigma-Aldrich, St. Louis, MO). ELISA kits were used for measurements of leptin (R&D Systems), insulin (DRG Diagnostics International Limited), and adiponectin (B-Bridge International) according to manufacturer's instructions.

### Preadipocytes isolation and culture

Preadipocyte isolation and culture from epididymal WAT and interescapular brown adipose tissue (BAT) were performed as described previously (17). The differentiation medium was supplemented with rosiglitazone ($10^{-7}$ mol/l; BRL) or vehicle (DMSO) in the indicated experiments.

### RNA preparation, ribonuclease protection assay, and real-time quantitative RT-PCR

Total RNA was isolated using RNAeasy kit (Qiagen) and STAT60 (Tel-text) for tissues samples according to the manufacturer's instructions. Ribonuclease protection assays (RPAs) were carried out as standard protocols (5). Isotopic bands were visualized by autoradiography and quantitated by PhosphoImager analysis using ImageQuant software (Molecular Dynamics, Sunnyvale, CA).

Real-time quantitative PCR was used to analyze RNA from tissues and primary cultures. Total RNA (500 ng) was reverse-transcribed as standard protocols. Real-time quantitative PCR was performed on TaqMan 7700/7900 Sequence Detection System (Applied Biosystems). Primers (online appendix) were designed using the Primer Express 2.0 software. 18S ribosomal RNA was used as control to normalize gene expression.

### Light microscopy, immunohistochemistry, and transmission electron microcopy

Tissue samples for morphological analysis were prepared according to published protocols (18). For light microscopy, sections were stained with hematoxylin-eosin. For immunolocalization of UCP-1 and tyrosine hydroxylase, sections from BAT samples were processed according to the avidin-biotin-peroxidase method (18). Electromicroscopy was performed as described previously (19).

### Oxygen consumption and body composition analysis

Oxygen consumption was measured in 12- to 24-week-old PPARγ2 knockout and wild-type mice by an OXYMAX System 4.93 indirect calorimeter (Columbus Instruments, Columbus, OH) as described previously (20). For body composition analysis, dual-energy X-ray absorptiometry (Lunar) was performed following the manufacturer's instructions.

### Magnetic resonance imaging

Magnetic resonance imaging (MRI) was performed at 9.4 Tesla using a volume coil. $T_1$-weighted multislice spin-echo (repetition time, 0.35 s; echo time, 6 ms; field of view, 3 × 3 $cm^2$, 512 × 512 matrix; slice thickness, 2 mm) and fat-selective three-dimensional spin-echo (repetition time, 0.2 s; echo time, 8 ms; field of view, 3 × 3 × 3.2 $cm^2$, 512 × 256 × 16 matrix zero-filled to 512 × 512 × 16; chemical shift selective pulse placed at 1.3 ppm) images were collected from five wild-type and five knockout animals. Regions of interest were manually delineated in each fat-selective image using $T_1$-weighted images as an additional reference. Background noise was removed by thresholding, and the number of fat pixels and their total signal intensity were calculated by summing the data from each slice. A percentage of selected fat region from total fat was calculated in each animal.

### Glucose tolerance test, insulin tolerance test, and euglycemic-hyperinsulinemic clamps on normal diet and HFD-fed mice

For the two diets tested, food was removed for 6 h before the initiation of a glucose tolerance test (GTT) (1 g glucose/kg body wt) or an insulin tolerance test (ITT) (0.75 U/kg insulin) (21). Blood glucose levels were monitored using a glucose meter (Boehringer) on 2.5-μl samples of tail. Glucose turnover analysis using euglycemic-hyperinsulinemic clamps was performed according to previously published protocols (21).

### Statistics

Results were expressed as means ± SE. Statistical analysis performed using a two-tailed unpaired *t* test between groups yielded *P* values less than 0.05. Kruskal-Wallis was used for analysis of the area of epididymal and subcutaneous WAT adipocytes.

## RESULTS

### Generation of PPARγ2 knockout mice

The mouse PPARγ gene spans >105 kilobases (kb) and is present as two isoforms, PPARγ1 and PPARγ2, which share six exons designated 1–6. The transcription of PPARγ1 is driven by an upstream promoter (P1) that also drives expression of two untranslated PPARγ1-

specific exons, A1 and A2. The additional amino acids at the $NH_2$ terminus of PPARγ2 are encoded by an additional exon B1, which is uniquely regulated by a separate promoter (P2). A targeting vector (see RESEARCH DESIGN AND METHODS) was designed for the production of germline knockout mice (PPARγ2 knockout) (Fig. 1*A*). Positively targeted clones for the disruption of exon B1 of the PPARγ2 gene were identified by Southern analysis (Fig. 1*B*) and PCR (Fig. 1*A*). Chimeric offspring were crossed to obtain heterozygotes as confirmed by PCR genotyping (Fig. 1*C*). Absence of the PPARγ2 isoform in PPARγ2 knockout mice was confirmed by RPA using total RNA from WAT and BAT (Fig. 1*D*). Normal PPARγ1 isoform expression was confirmed in subcutaneous WAT and BAT (Fig. 1*E*), as well as skeletal muscle and liver (data not shown). Breeding of animals heterozygous for the deleted allele produced litters that did not deviate from the expected Mendelian ratio of genotypes (average number of pups in each litter $n = 7.5$). PPARγ2 knockout animals bred normally and were physically indistinguishable from wild-type or heterozygous littermates.

## Food intake, energy expenditure, and body composition of PPARγ2 knockout mice

The ablation of PPARγ2 did not result in a major metabolic phenotype. As shown in Fig. 2*A*, the growth curves of male PPARγ2 knockout, heterozygous, and wild-type mice fed a normal diet for 24 weeks are similar. No differences in food intake at 12 weeks in males (Fig. 2*B*) or females from any of the genotypes were observed. Moreover, no differences were observed in oxygen consumption between the knockout and wild-type mice ($65.4 \pm 3.0$ vs. $61.4 \pm 1.8$ ml $\cdot$ kg$^{-1}$ $\cdot$ min$^{-1}$, $n = 9$–10), and dual-energy X-ray absorptiometry analysis of body composition in mice fed a normal diet revealed that at age 16 or 32 weeks, PPARγ2 knockout mice had similar lean body and total fat mass to wild-type mice (Fig. 2*C*).

**Characterization of the adipose tissues of the PPARγ2 knockout mouse—** Histological analysis of WAT from PPARγ2 knockout and wild-type littermates fed normal diet showed similar adipocyte size or number in both genotypes (Fig. 3*A*). MRI demonstrated preferential deposition of fat in the subcutaneous fat pad of the PPARγ2 knockout mice without a decrease in the intra-abdominal/perigonadal fat pad. Because total body fat content was similar in wild-type and knockout mice, we investigated the fat content of other adipose tissue depots. We found decreased intradermal fat deposition at 16 (data not shown) and 32 weeks (Fig. 2*D*). The latter aspect was further confirmed by histological analysis (online appendix).

**PPARγ2-deficient white preadipocytes fail to differentiate in vitro—**We investigated whether PPARγ2-deficient preadipocytes could differentiate in vitro. Despite normal differentiation of adipose tissue in vivo, preadipocytes from WAT of PPARγ2 knockout mice were poorly differentiated in vitro (Fig. 3*C* and *D*). Expression of the adipocyte-specific marker aP2 in the knockout cultures was markedly decreased during the whole protocol of differentiation (data not shown), indicating that adipogenesis was impaired in vitro. Rosiglitazone treatment partially rescued their differentiation to levels comparable with untreated wild-type preadipocytes (Fig. 3*E*).

**Gene expression analysis of PPARγ2-deficient WAT—**The lack of PPARγ2 was associated with a 50% decrease in the expression of PPARγ target genes such as lipoprotein

lipase, aP2, perilipin, and Glut4 in WAT from PPARγ2 knockout mice fed a normal diet (Fig. 4*A*). We also found that the expression of pro-oxidative genes such as PPARα, long-chain acyl CoA dehydrogenase, and PGC1α were decreased in WAT from PPARγ2 knockout mouse (Fig. 4*A*). No changes in PPARδ gene expression were observed. We also assessed the expression of genes involved in de novo lipogenesis. Sterol regulatory element–binding protein 1c (SREBP1c) and fatty acid synthase were significantly decreased in WAT of PPARγ2 knockout mice fed a normal diet (Fig. 4*A*).

**Altered lipid composition of WAT deficient in PPARγ2—**We were intrigued by the normal appearance of the WAT of the PPARγ2 knockout mouse in vivo despite changes in gene expression of lipogenic and β-oxidative genes and marked impairment of in vitro differentiation. For this reason, we investigated whether ablation of PPARγ2 was associated with changes in adipose tissue lipid composition. We studied subcutaneous WAT from mice fed a normal diet using liquid chromatography/mass spectrometry (LC/MS) (Fig. 5 and online appendix; methods described in detail in online appendix). Although the total lipid content in adipose tissue is similar in wild-type and PPARγ2 knockout mice, Fig. 5 shows that qualitative differences exist between both models, as indicated by the number of specific lipid species upregulated and downregulated in wild-type and knockout animals. The lipid profile of WAT from PPARγ2 knockout mice revealed downregulation of long-chain triacylglycerol species and upregulation of a cluster of lipids, containing short-chain triacylglycerols, long-chain phospholipids, lyso-phospholipids, and diacylglycerols. We also found a downregulated cluster of C32:n phosphatidylcholines and an upregulated cluster of ceramide-related compounds. The latter were found at a concentration three orders of magnitude lower than triglyceride species and were all approximately two-fold upregulated in the WAT of PPARγ2 knockout versus wild-type mice ($P < 0.05$). Using correlation network analysis (22), we identified specific clusters lipid species that represent qualitative differences in their composition (online appendix).

**PPARγ2 is not required for BAT development and function in vivo—**In mice housed at ambient temperature and fed normal diet or HFD, there was no difference in rectal temperature between genotypes. Histological analysis and electron microscopy (online appendix) showed no differences in cellularity, mitochondrial content, or structure between the genotypes. Immunohistochemical analysis using antibodies against UCP-1, the BAT-specific thermogenic protein, and tyrosine hydroxylase, a specific marker of noradrenergic nerve fibers, did not show differences between genotypes (online appendix). These results were confirmed by gene expression analysis that showed similar levels for UCP-1 and UCP-2 mRNA in BAT from both genotypes. Similarly, the expression of genes involved in fatty acid synthesis, such as SREBP1c and PPARγ1, were unchanged as was the expression of genes involved in β-oxidation (e.g., PPARα) or mitochondrial biogenesis (e.g., PGC1α) (data not shown).

## Characterization of insulin sensitivity in PPARγ2 knockout mice

**Genetic ablation of PPARγ2 induces insulin resistance—**Fasted glucose levels were significantly increased in the presence of moderately increased plasma insulin levels (Table 1) in the PPARγ2 knockout mouse. GTTs performed in 16-week-old male and female

mice fed normal diet revealed glucose intolerance in PPARγ2 knockout male mice, but not in females (Fig. 6*A*). No substantial differences were detected in plasma levels of triglycerides and fatty acids (Table 1). To further characterize this phenotype, euglycemic-hyperinsulinemic clamps were performed in age-matched male PPARγ2 knockout and wild-type mice. Whole-body glucose turnover rates were determined using high (18 mU · $kg^{-1}$ · $min^{-1}$) rates of insulin infusion. As shown in Fig. 6*C*, insulin-increased glucose turnover, glucose infusion rates, and whole-body glycogen synthesis were decreased in PPARγ2 knockout mice. Insulin suppressed hepatic endogenous glucose production similarly in both genotypes. Altogether, these data indicate a state of peripheral insulin resistance in the PPARγ2 knockout mice with no alteration in hepatic glucose production, at least at high plasma insulin concentrations.

To investigate potential mediators of insulin resistance in PPARγ2 knockout mice, we measured gene expression and plasma levels of adipokines involved in insulin sensitivity. PPARγ2 knockout mice had a 40% reduction in adiponectin mRNA levels in WAT (Fig. 4*A*) and a similar reduction in adiponectin levels in plasma compared with wild-type mice receiving a normal diet (Table 1). In addition, plasma adiponectin levels in females were 50% higher than in males in both genotypes (female wild type vs. male wild type, 31.0 ± 2.6 vs. 15.2 ± 1.2; female knockout vs. male knockout, 16.3 ± 2.7 vs.7.9 ± 1.2). Interestingly, mice lacking PPARγ2 not only had normal morphological adipose tissue differentiation in vivo but also increased leptin plasma levels. No differences were observed in plasma levels of resistin (Fig. 6*D*).

**Lipotoxicity and insulin resistance in the PPARγ2 knockout mouse—**We investigated whether the insulin resistance in the PPAR γ2 knockout mouse was associated with ectopic deposition of lipids. Histological analysis of muscle and liver from PPAR γ2 knockout mice fed normal diet did not reveal microscopic evidence of fat accumulation (data not shown). Levels of triglycerides in skeletal muscle as determined by LC/MS were low in both genotypes. Gene expression analysis of liver (data not shown) and skeletal muscle (Fig. 7*D*) from wild-type and PPARγ2 knockout mice fed normal diet did not reveal differences in genes involved either in β-oxidation (PPARα and PPARδ) or lipogenesis.

## PPARγ2 knockout mice fed an HFD have similar levels of insulin resistance to wild-type littermates

We proceeded to examine how the absence of PPARγ2 might modulate the metabolic effects of high-fat feeding. No differences in body weight (Fig. 2*A*), body composition (Fig. 2*C*), food intake, or oxygen consumption were observed during HFD. Histological analysis of epididymal and subcutaneous adipose depots from HFD-fed PPARγ2 knockout mice revealed adipocyte hypertrophy (Fig. 3*A* and *B*) and preferential deposition of fat in the subcutaneous depot. Similar to normal diet, the adipose tissue of the PPARγ2 knockout fed an HFD had decreased levels of prolipogenic target genes including perilipin, fatty acid synthase, and SREBP1c (Fig. 4*B*).

After 28 weeks of an HFD, there was a significant rise in basal glucose (wild-type HFD vs. wild-type normal diet, 229 ± 14.1 vs.109 ± 11.1 mg/dl) and insulin levels in wild-type mice

compared with similarly aged mice fed on normal diet (wild-type HFD vs. wild-type normal diet, 1.20 ± 0.06 vs. 0.47 ± 0.13 μg/l). We performed GTTs and ITTs (Fig. 6*B*), which indicated insulin resistance but no differences between genotypes. These results were further confirmed with euglycemic-hyperinsulinemic glucose clamps that showed a similar degree of insulin resistance in wild-type and PPARγ2 knockout mice after long-term HFD (Fig. 6*C*). More interestingly, the degree of insulin resistance in the PPARγ2 knockout mice fed an HFD was no worse than the degree of insulin resistance with a normal diet.

Consistent with the insulin resistance phenotype observed in the PPARγ2 knockout mice fed a normal diet, levels of Glut4 and insulin receptor substrate 1 (IRS1) mRNA were decreased in WAT (Fig. 7*A* and *B*). In response to HFD, levels of Glut4 and IRS1 decreased in the WAT of wild-type mice; however, in the WAT of PPARγ2 knockout mice, Glut4 and IRS1 levels did not decrease further. Analysis of skeletal muscle revealed no differences in Glut4 and IRS1 between wild-type and PPARγ2 knockout mice fed a normal diet. However, on an HFD, levels of Glut4 decreased in skeletal muscle of wild-type mice, whereas Glut4 levels remained at normal levels in the PPARγ2 knockout mice. Of interest, HFD increased mRNA levels of PPARγ2 in skeletal muscle of wild-type mice (wild-type normal diet vs. wild-type HFD, 1.21 ± 0.31 vs. 4.21 ± 0.77; $P < 0.01$) (Fig. 7*C*). These results suggest that induction of PPARγ2 in skeletal muscle may be required to mediate HFD-induced insulin resistance.

We investigated alterations in other potential modulators of insulin sensitivity that could account for the effect of PPARγ2 deficiency on high-fat feeding–induced insulin resistance. No differences in plasma fatty acid levels were observed. As with a normal diet, leptin levels were increased but to a further extent in the PPARγ2 knockout mouse compared with the wild-type mouse fed 28 weeks of an HFD (Fig. 6*D*). More interestingly, adiponectin levels were reduced in response to HFD in wild-type mice but were not further decreased in the similarly aged PPARγ2 knockout mice (wild-type normal diet vs. wild-type HFD, 14.8 ± 1.48 vs. 9.52 ± 1.07; $P < 0.05$; knockout normal diet vs. knockout HFD, 7.73 ± 1.42 vs. 7.85 ± 1.63; NS).

## DISCUSSION

The PPARγ2 knockout mouse is viable and born at the expected Mendelian ratios, indicating that PPARγ2 is not required for normal gestation. Contrary to the recently published PPARγ2 knockout model of Zhang et al. (16), our PPARγ2 knockout model does not result in any obvious impairment in the development of WAT and BAT under normal nutritional conditions. Yet, despite similar weight, body composition, food intake, and energy balance, the male PPARγ2 knockout mice are more insulin resistant when fed a regular diet than wild-type animals. Thus, the effect of PPARγ2 on insulin sensitivity is not due to any impairment of adipocyte differentiation in vivo but rather a direct effect of this isoform on insulin sensitivity.

We provide evidence that the PPARγ2 knockout mice store similar amounts of excess of fat compared with wild-type animals when provided a hypercaloric diet but do so by the production of hypertrophied adipocytes. However, HFD does not make the insulin resistance worse, despite marked adipocyte hypertrophy and decreased adipocyte expression of PPARγ

target genes. This raises the intriguing notion that PPARγ2 may be required to mediate the adverse effects of an HFD on carbohydrate metabolism. Furthermore, because PPARγ2-deficient preadipocytes hardly differentiate in vitro, a robust compensatory mechanism is likely to exist in vivo to promote adipogenesis in the absence of PPARγ2.

We consider it unlikely that adipocyte hypertophy in response to HFD is caused by a reduction in gene dosage, because PPARγ heterozygous animals, which have the same amount of total PPARγ in adipose tissue as PPARγ2 knockout animals, have adipocyte hyperplasia and maintained insulin sensitivity in response to high-fat feeding (11,23). Also, PPARγ1 expression in adipose tissue is not increased in our PPARγ2 knockout mice with an HFD, so it is unlikely this could act as a compensatory mechanism for the lack of PPARγ2, although an increase in activation dependent on increased ligand availability cannot be ruled out. This suggests that each PPARγ isoform may have different functions and/or potency, and that their relative expression may determine the balance between growth (facilitated predominantly by γ1), differentiation (facilitated predominantly by γ2), and insulin sensitivity (facilitated predominantly by γ2). We do not have a clear explanation for the differences in WAT development between both PPARγ2 knockout models. It is intriguing that the PPARγ2 knockout model of Zhang et al. (16) appears similar to the adipose tissue-specific global PPARγ knockout (13) or the severely hypomorphic PPARγ mouse (9), both having different degrees of lypodystrophy and reduced serum leptin due to a lack of both PPARγ1 and PPARγ2 isoforms. In contrast to these models, the adipose tissue of our PPARγ2 knockout mouse does not have any sign of lipodistrophy and even produces increased leptin levels compared with the wild-type mice. One possibility that cannot be discounted is that the differences in phenotype may be in part due to the fact that Zhang's model is enriched for C57/Bl6 background, whereas our mouse is enriched for 129 background.

Given the normal appearance of the WAT in vivo despite its altered gene expression pattern and poor differentiation in vitro, we investigated the nature of the lipid species accumulated in the WAT. MS analysis revealed that the PPARγ2 knockout mice had reduced levels of long-chain triglycerides in WAT, however, the total lipid mass of the adipose tissue was conserved as a result of increased accumulation of other lipid species such as short-chain triglycerides, diacylglycerols, phospholipids, and rare ceramide species. These results suggest that the absence of PPARγ2 resulted in qualitative alterations in the lipid composition of the adipose tissue. Of interest, some of these phospholipid species accumulated in the adipose tissue of the PPARγ2 knockout mouse may act as potential PPARγ ligands (24,25) that may facilitate adipocyte differentiation in vivo. In support of this possibility is the fact that rosiglitazone, a member of the thiazolidinedione class of insulin-sensitizing drugs that bind and activate PPARγ, can partially rescue the differentiation of PPARγ2-deficient preadipocytes. Yamauchi et al. (23) have suggested that mice heterozygous for a global PPARγ null mutation (50% of PPARγ gene dosage at the expense of both isoforms) were protected from insulin resistance, both basally and after high-fat feeding, because they have higher plasma leptin levels, which they related to the presence of larger numbers of smaller fat cells in this animal model. Our data contrast with this interpretation somewhat because our PPARγ2 knockout (50% of PPARγ gene dosage in adipose tissue at the expense of PPARγ2 exclusively) animals were insulin resistant in the

normal diet–fed state despite the presence of elevated plasma leptin levels. However, because the increase in leptin is more marked, in absolute terms, during high-fat feeding, it can be argued that leptin may still play a protective role in the PPARγ2 knockout mouse. Interestingly, Zhang et al.'s PPARγ2 knockout mouse (50% of PPARγ gene dosage at the expense of PPARγ2 exclusively) shows poorly differentiated adipose tissue and negligible levels of leptin.

An unexpected finding was that although male PPARγ2 knockout mice are insulin resistant on normal diet, they do not become more insulin resistant on an HFD. In contrast to the progressive deterioration of insulin sensitivity seen in wild-type mice after 28 weeks of HFD, insulin sensitivity in PPARγ2 knockout mice as assessed by euglycemic-hyperinsulinemic clamp did not further deteriorate. How might the absence of PPARγ2 abrogate the normal effect of high-fat feeding to worsen insulin sensitivity? One possible explanation relates to the fact that PPARγ2 knockout animals were already insulin resistant on a normal diet. It is possible that the molecular mechanisms whereby PPARγ2 deficiency leads to insulin resistance on the normal diet are very similar to the mechanism whereby high-fat feeding impairs insulin sensitivity, and therefore no additive effects are observed.

The most compelling link between PPARγ2 ablation, adipokines, and insulin resistance was the 50% decrease in plasma adiponectin levels observed in PPARγ2 knockout mice fed a normal diet. Adiponectin levels in plasma decreased progressively (as indicated by data at 12 and 28 weeks of HFD) in wild-type mice in response to HFD, whereas they remained stable at low levels in the PPARγ2 knockout mouse. Thus, adiponectin plasma levels were the best correlate between dietary treatments and changes in insulin sensitivity in wild-type and PPARγ2 knockout mice. Because adiponectin levels did not decrease further in response to HFD in the PPARγ2 knockout mice, it can be speculated that PPARγ2 may be involved in the mechanisms mediating HFD-induced insulin resistance through its effects on the regulation of adiponectin. As previously reported (26), we also observed that males had 50% less plasma adiponectin levels than females in both genotypes. Thus, female protection against insulin resistance observed in the PPARγ2 knockout mice may be, at least in part, mediated by sex-related differences in adiponectin levels. Finally plasma levels of fatty acids and resistin were not increased in the plasma of the PPARγ2 knockout mice.

An alternative possibility may be that PPARγ2 induction in skeletal muscle in response to an HFD was required to develop diet-induced insulin resistance. This is supported by our data showing that an HFD induces PPARγ2 gene expression in skeletal muscle of wild-type mice. Also, in the absence of PPARγ2 induction in skeletal muscle, an HFD challenge results in upregulation of the PPARα/δ target gene expression program of fatty acid oxidation (PGC-1α, UCP-2, and PPARδ), which may contribute to prevent lipotoxicity-induced insulin resistance. The possibility that decreased PPARγ2 levels may facilitate the activity of other pro-oxidative PPARs is also supported by our recent observation that dominant-negative forms of PPARγ and PPARα are capable of interfering with other PPAR signaling (27).

The relevance of skeletal muscle for the effects of an HFD on insulin resistance is also suggested by the specific changes observed in Glut4 expression. With a normal diet we

found that Glut4 and IRS1 expression was unaltered in the skeletal muscle of the PPARγ2 knockout mice, suggesting that other tissues may be involved in the insulin resistance seen in these animals. Fed an HFD, the PPARγ2 knockout animals did not become more insulin resistant, unlike the wild-type animals whose insulin sensitivity decreased to a level similar to that in the knockout animals. The expression levels of IRS1 and Glut4 in the muscle of the wild-type animals fell, matching the reduction in insulin sensitivity, whereas in the knockout animals, the expression levels were maintained. This suggests that the expression of PPARγ2 in muscle may cause HFD-related insulin resistance.

In conclusion, we have shown that changes in the relative expression of PPARγ1 and PPARγ2 may cause depot-specific adipose tissue hypertrophy or hyperplasia in vivo. PPARγ2 is also required to maintain normal insulin sensitivity and may be involved in mediating HFD-induced insulin resistance. Our results indicate that with an HFD, PPARγ2 null mice have marked adipocyte hypertrophy but no worse insulin resistance than wild-type littermates with normal-sized adipocytes. This suggests that the idea of PPARγ activity positively influencing insulin sensitivity by promoting increased numbers of small adipocytes is overly simplistic. Our results underscore the relevance of the adipokine repertoire and ectopic PPARγ2 expression to diet-induced insulin resistance.

## Supplementary Material

Refer to Web version on PubMed Central for supplementary material.

## ACKNOWLEDGMENTS

A.V.-P. has received support from Wellcome Trust Integrative Physiology program and MRC Career Establishment Grant.

We greatly appreciate the technical assistance of Keith Burling, Kate Day, Gemini Bevan, Janice Carter, Sylvia Shelton, and John-Paul Whiting.

## Glossary

| | |
|---|---|
| **BAT** | brown adipose tissue |
| **GTT** | glucose tolerance test |
| **HFD** | high-fat diet |
| **ITT** | insulin tolerance test |
| **IRS1** | insulin receptor substrate 1 |
| **LC/MS** | liquid chromatography/mass spectrometry |
| **MRI** | magnetic resonance imaging |
| **PPARγ** | peroxisome proliferator–activated receptor-γ |
| **RPA** | ribonuclease protection assay |
| **SREBP1c** | sterol regulatory element–binding protein 1c |
| **WAT** | white adipose tissue |

## REFERENCES


1. Escher P, Braissant O, Basu-Modak S, Michalik L, Wahli W, Desvergne B. Rat PPARs: quantitative analysis in adult rat tissues and regulation in fasting and refeeding. Endocrinology. 2001; 142:4195–4202. [PubMed: 11564675]
2. Werman A, Hollenberg A, Solanes G, Bjorbaek C, Vidal-Puig AJ, Flier JS. Ligand-independent activation domain in the N terminus of peroxisome proliferator-activated receptor γ (PPARγ): differential activity of PPARγ1 and -2 isoforms and influence of insulin. J Biol Chem. 1997; 272:20230–20235. [PubMed: 9242701]
3. Ren D, Collingwood TN, Rebar EJ, Wolffe AP, Camp HS. PPARγ knockdown by engineered transcription factors: exogenous PPARγ2 but not PPARγ1 reactivates adipogenesis. Genes Dev. 2002; 16:27–32. [PubMed: 11782442]
4. Altshuler D, Hirschhorn JN, Klannemark M, Lindgren CM, Vohl MC, Nemesh J, Lane CR, Schaffner SF, Bolk S, Brewer C, Tuomi T, Gaudet D, Hudson TJ, Daly M, Groop L, Lander ES. The common PPARγ Pro12Alapolymorphism is associated with decreased risk of type 2 diabetes. Nat Genet. 2000; 26:76–80. [PubMed: 10973253]
5. Vidal-Puig A, Jimenez-Linan M, Lowell BB, Hamann A, Hu E, Spiegelman B, Flier JS, Moller DE. Regulation of PPAR γ gene expression by nutrition and obesity in rodents. J Clin Invest. 1996; 97:2553–2561. [PubMed: 8647948]
6. Cock TA, Houten SM, Auwerx J. Peroxisome proliferator-activated receptor-γ: too much of a good thing causes harm. EMBO Rep. 2004; 5:142–147. [PubMed: 14755307]
7. Barak Y, Nelson MC, Ong ES, Jones YZ, Ruiz-Lozano P, Chien KR, Koder A, Evans RM. PPAR γ is required for placental, cardiac, and adipose tissue development. Mol Cell. 1999; 4:585–595. [PubMed: 10549290]
8. Rosen ED, Sarraf P, Troy AE, Bradwin G, Moore K, Milstone DS, Spiegelman BM, Mortensen RM. PPAR γ is required for the differentiation of adipose tissue in vivo and in vitro. Mol Cell. 1999; 4:611–617. [PubMed: 10549292]
9. Koutnikova H, Cock TA, Watanabe M, Houten SM, Champy MF, Dierich A, Auwerx J. Compensation by the muscle limits the metabolic consequences of lipodystrophy in PPAR γ hypomorphic mice. Proc Natl Acad Sci U S A. 2003; 100:14457–14462. [PubMed: 14603033]
10. Spiegelman BM. PPAR-γ: adipogenic regulator and thiazolidinedione receptor. Diabetes. 1998; 47:507–514. [PubMed: 9568680]
11. Kubota N, Terauchi Y, Miki H, Tamemoto H, Yamauchi T, Komeda K, Satoh S, Nakano R, Ishii C, Sugiyama T, Eto K, Tsubamoto Y, Okuno A, Murakami K, Sekihara H, Hasegawa G, Naito M, Toyoshima Y, Tanaka S, Shiota K, Kitamura T, Fujita T, Ezaki O, Aizawa S, Kadowaki T, et al. PPAR γ mediates high-fat diet-induced adipocyte hypertrophy and insulin resistance. Mol Cell. 1999; 4:597–609. [PubMed: 10549291]
12. Miles PD, Barak Y, He W, Evans RM, Olefsky JM. Improved insulin-sensitivity in mice heterozygous for PPAR-γ deficiency. J Clin Invest. 2000; 105:287–292. [PubMed: 10675354]
13. He W, Barak Y, Hevener A, Olson P, Liao D, Le J, Nelson M, Ong E, Olefsky JM, Evans RM. Adipose-specific peroxisome proliferator-activated receptor γ knockout causes insulin resistance in fat and liver but not in muscle. Proc Natl Acad Sci U S A. 2003; 100:15712–15717. [PubMed: 14660788]
14. Norris AW, Chen L, Fisher SJ, Szanto I, Ristow M, Jozsi AC, Hirshman MF, Rosen ED, Goodyear LJ, Gonzalez FJ, Spiegelman BM, Kahn CR. Muscle-specific PPARγ-deficient mice develop increased adiposity and insulin resistance but respond to thiazolidinediones. J Clin Invest. 2003; 112:608–618. [PubMed: 12925701]
15. Hevener AL, He W, Barak Y, Le J, Bandyopadhyay G, Olson P, Wilkes J, Evans RM, Olefsky J. Muscle-specific Pparg deletion causes insulin resistance. Nat Med. 2003; 9:1491–1497. [PubMed: 14625542]
16. Zhang J, Fu M, Cui T, Xiong C, Xu K, Zhong W, Xiao Y, Floyd D, Liang J, Li E, Song Q, Chen YE. Selective disruption of PPARγ2 impairs the development of adipose tissue and insulin sensitivity. Proc Natl Acad Sci U S A. 2004; 101:10703–10708. [PubMed: 15249658]

17. Sewter CP, Blows F, Vidal-Puig A, O'Rahilly S. Regional differences in the response of human pre-adipocytes to PPARγ and RXRα agonists. Diabetes. 2002; 51:718–723. [PubMed: 11872672]
18. De Matteis R, Ricquier D, Cinti S. TH-, NPY-, SP-, and CGRP-immunoreactive nerves in interscapular brown adipose tissue of adult rats acclimated at different temperatures: an immunohistochemical study. J Neurocytol. 1998; 27:877–886. [PubMed: 10659680]
19. Cinti S, Zancanaro C, Sbarbati A, Cicolini M, Vogel P, Ricquier D, Fakan S. Immunoelectron microscopical identification of the uncoupling protein in brown adipose tissue mitochondria. Biol Cell. 1989; 67:359–362. [PubMed: 2620168]
20. Vidal-Puig AJ, Grujic D, Zhang CY, Hagen T, Boss O, Ido Y, Szczepanik A, Wade J, Mootha V, Cortright R, Muoio DM, Lowell BB. Energy metabolism in uncoupling protein 3 gene knockout mice. J Biol Chem. 2000; 275:16258–16266. [PubMed: 10748196]
21. Burcelin R, Crivelli V, Dacosta A, Roy-Tirelli A, Thorens B. Heterogeneous metabolic adaptation of C57BL/6J mice to high-fat diet. Am J Physiol Endocrinol Metab. 2002; 282:E834–E842. [PubMed: 11882503]
22. Clish CB, Davidov E, Oresic M, Plasterer TN, Lavine G, Londo T, Meys M, Snell P, Stochaj W, Adourian A, Zhang X, Morel N, Neumann E, Verheij E, Vogels JT, Havekes LM, Afeyan N, Regnier F, van der Greef J, Naylor S. Integrative biological analysis of the APOE*3-leiden transgenic mouse. Omics. 2004; 8:3–13. [PubMed: 15107233]
23. Yamauchi T, Kamon J, Waki H, Murakami K, Motojima K, Komeda K, Ide T, Kubota N, Terauchi Y, Tobe K, Miki H, Tsuchida A, Akanuma Y, Nagai R, Kimura S, Kadowaki T. The mechanisms by which both heterozygous peroxisome proliferator-activated receptor γ (PPARγ) deficiency and PPARγ agonist improve insulin resistance. J Biol Chem. 2001; 276:41245–41254. [PubMed: 11533050]
24. Davies SS, Pontsler AV, Marathe GK, Harrison KA, Murphy RC, Hinshaw JC, Prestwich GD, Hilaire AS, Prescott SM, Zimmerman GA, McIntyre TM. Oxidized alkyl phospholipids are specific, high affinity peroxisome proliferator-activated receptor γ ligands and agonists. J Biol Chem. 2001; 276:16015–16023. [PubMed: 11279149]
25. Nosjean O, Boutin JA. Natural ligands of PPARγ: are prostaglandin $J_2$ derivatives really playing the part? Cell Signal. 2002; 14:573–583. [PubMed: 11955950]
26. Cnop M, Havel PJ, Utzschneider KM, Carr DB, Sinha MK, Boyko EJ, Retzlaff BM, Knopp RH, Brunzell JD, Kahn SE. Relationship of adiponectin to body fat distribution, insulin sensitivity and plasma lipoproteins: evidence for independent roles of age and sex. Diabetologia. 2003; 46:459–469. [PubMed: 12687327]
27. Semple RK, Meirhaeghe A, Vidal-Puig AJ, Schwabe JW, Wiggins D, Gibbons GF, Gurnell M, Chatterjee VK, O'Rahilly S. A dominant negative human peroxisome proliferator-activated receptor (PPAR)$_\alpha$ is a constitutive transcriptional co-repressor and inhibits signaling through all PPAR isoforms. Endocrinology. 2005; 146:1871–1882. [PubMed: 15661858]

Europe PMC Funders Author Manuscripts

Europe PMC Funders Author Manuscripts

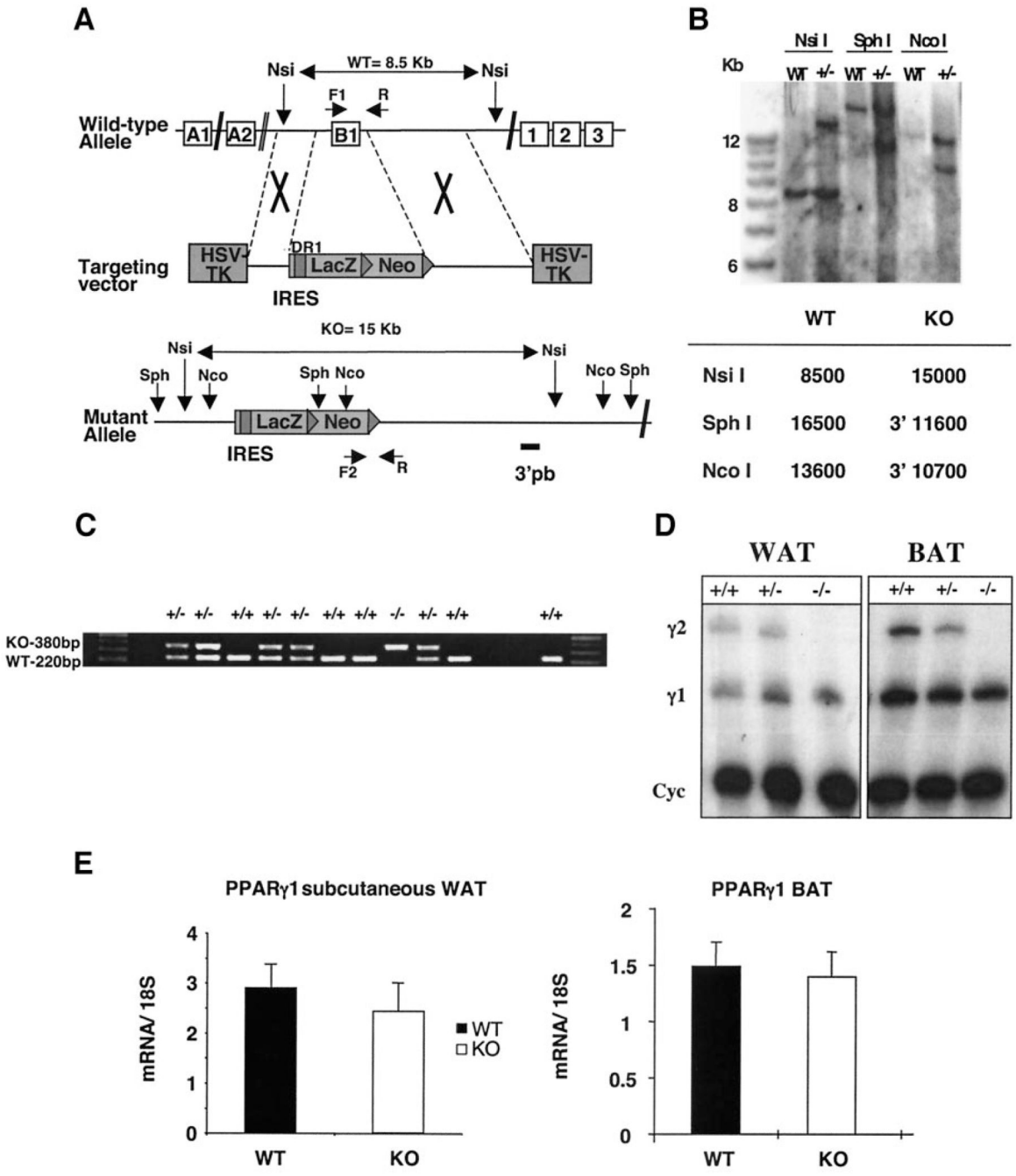


**FIG. 1.**

Generation of PPARγ2 knockout mouse. *A*: Schematic representation of PPARγ2 knockout targeting construct and the predicted structure of the recombinant allele. The targeting construct contains 5.2 kb of homologous mouse PPARγ2 genomic DNA, with LacZ/NEO cassette of 5.335 kb. The LacZ/NEO cassette replaces ~164 bp of the PPARγ locus including all 145 bp of exon B1. *B*: Southern blot analysis of genomic DNA. The 3′ probe (3′pb) is located outside the targeting construct sequence. Genomic DNA was digested with *Nsi*I, *Sph*I, and *Nco*I. *C*: Genotyping was performed by multiplex PCR in the same reaction.

Specific primers used to detect the knockout (KO) allele were the sense Asc 306 (F2), located in the NEO cassette and PPAR antisense (R) located 42 bp downstream of exon B1 (380-bp PCR product). Primers used to detect the wild-type (WT) allele were the PPAR sense (F1) located 7 bp upstream of exon B1 and PPAR antisense (R) (220-bp PCR product). The binding site for primer F1 was deleted by homologous recombination. *D*: RPA analysis of PPARγ1 and PPARγ2 in wild-type, heterozygous, and PPARγ2 knockout mice using total RNA from WAT and BAT. Cyc, cyclophilin. *E*: TaqMan analysis of PPARγ1 in wild-type and PPARγ2 knockout mouse subcutaneous WAT and interscapular BAT.



Europe PMC Funders Author Manuscripts

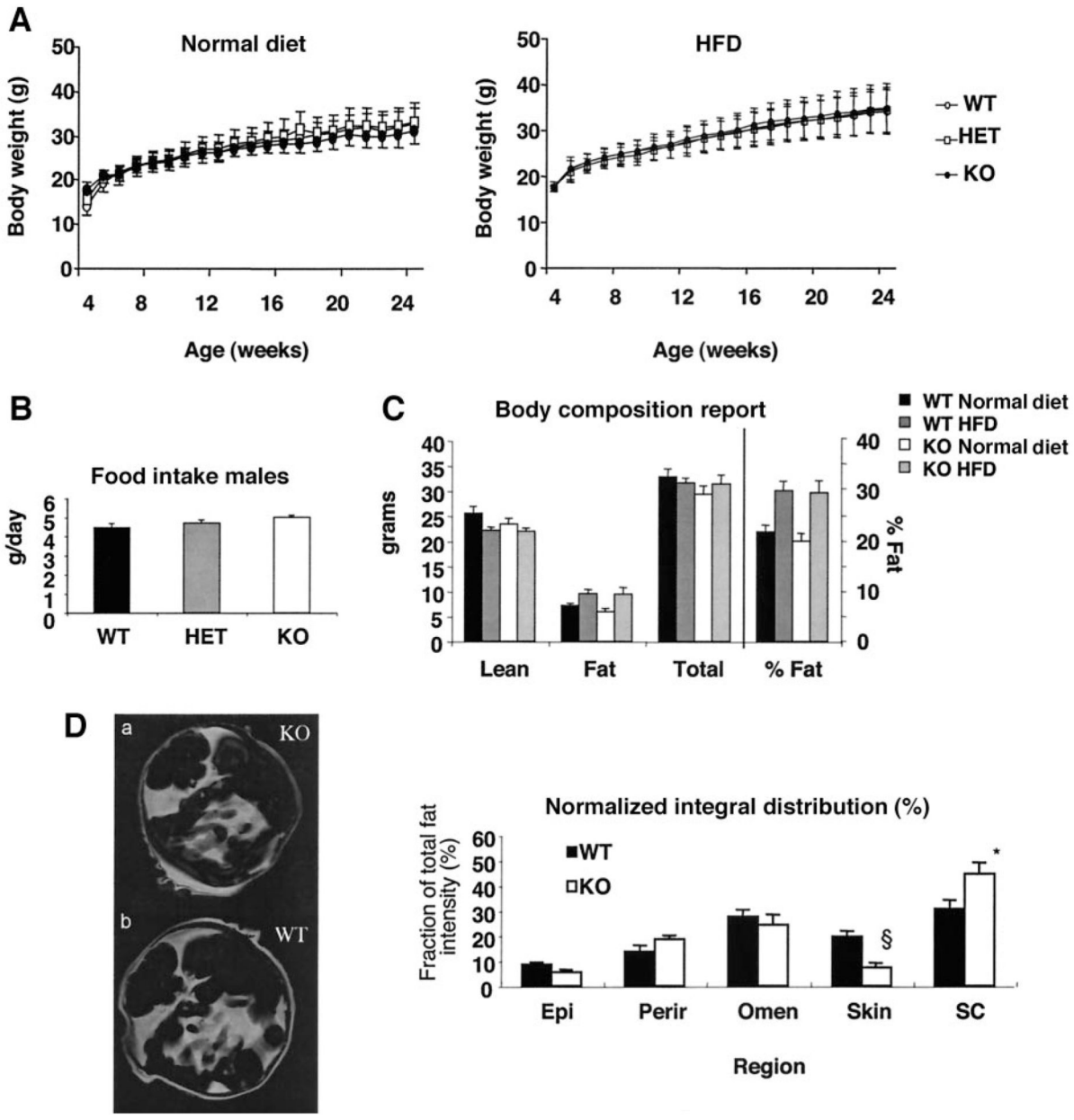


**FIG. 2.**

Physiological characterization of PPARγ2 knockout mouse. *A*: Body weights of males (○, wild type; □, heterozygous; •, PPARγ2 knockout; $n = 20$) fed a normal diet (*left*) or an HFD (*right*). *B*: Food intake from 20-week normal diet–fed mice ($n = 7$). *C*: Body composition analysis from 32-week-old male wild-type and PPARγ2 knockout mice fed a normal diet and a 28-week HFD ($n = 5$). *D*: Fat-selective MRI from 32-week-old male PPARγ2 knockout (*a*) and wild-type (*b*) mice ($n = 5$). Regions of interest (epididymal WAT [Epi], perirenal WAT [Perir], omental WAT [oMen], skin, subcutaneous WAT [SC]) were delineated in each fat-selective image, and their total signal intensity was calculated by summing the data from each slice. The results are expressed as a percentage of each fat region from total fat. KO, knockout; WT, wild type. *$P < 0.05$; §$P < 0.01$.

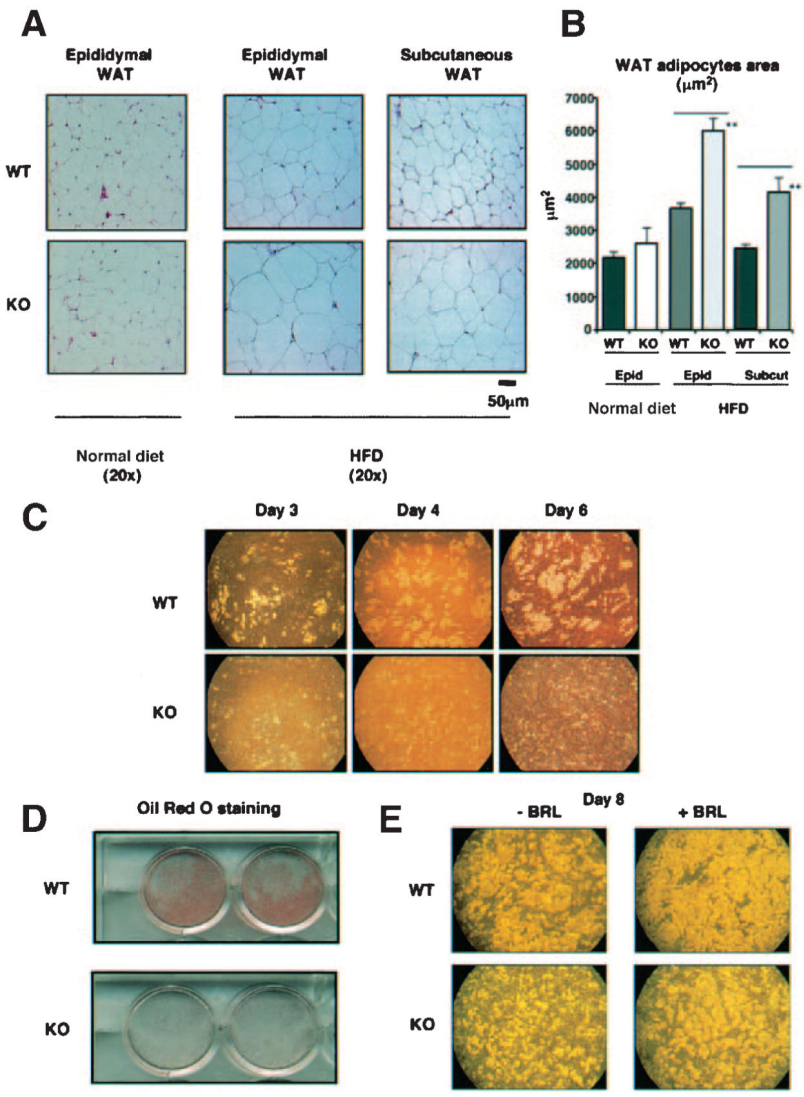


**FIG. 3.**

Characterization of the WAT of PPARγ2 knockout mice. *A*: Representative histological appearance of hematoxylin-eosin–stained sections from epididymal WAT, from male wild-type and PPARγ2 knockout mice fed a normal diet ($n = 7$), and from epididymal and subcutaneous WAT depots from mice fed a 16-week HFD ($n = 5$). *B*: Area of epididymal and subcutaneous WAT adipocytes (200 random adipocytes) from wild-type and PPARγ2 knockout mice fed a normal diet and an HFD ($n = 5$). $^{**}P < 0.01$ (Kruskal-Wallis test). *C*: Time course of WAT preadipocyte differentiation from wild-type and PPARγ2 knockout mice. Cells were observed by light microscopy after 3, 4, and 6 days of differentiation with standard differentiation-induction medium (representative experiment of three). *D*: Oil Red O staining of WAT adipocytes after 8 days of differentiation from wild-type and PPARγ2 knockout mice. *E*: 8 days of differentiation of WAT preadipocytes from wild-type and PPARγ2 knockout mice with and without BRL treatment.

Europe PMC Funders Author Manuscripts

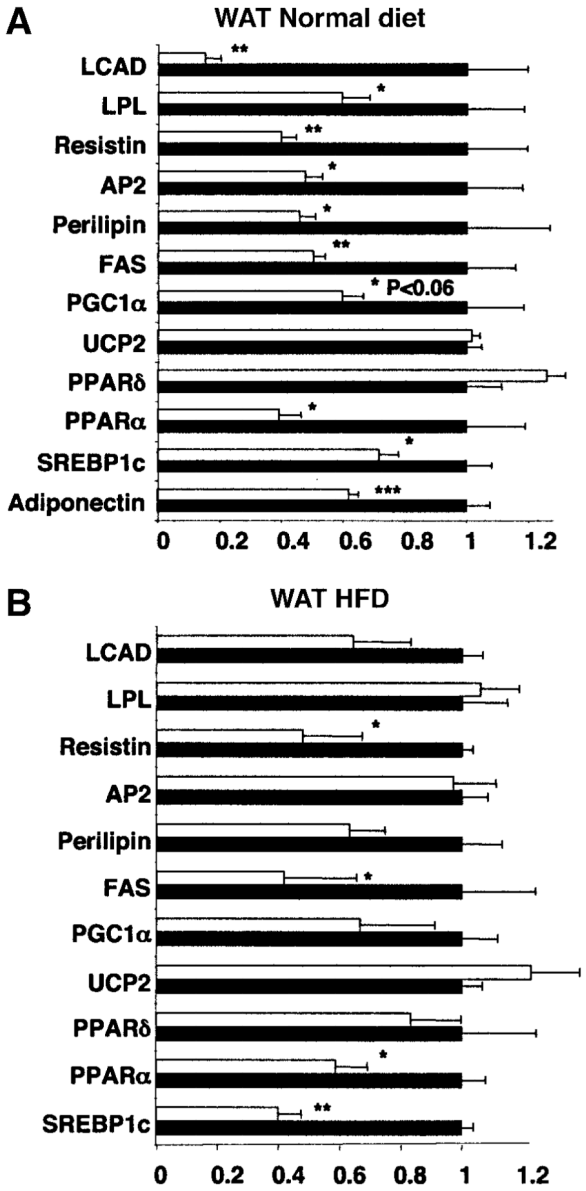


**FIG. 4.**

Gene expression analysis of PPARγ2-deficient WAT. Adipose tissue mRNA levels determined by real-time PCR of different genes from 16-week-old male wild-type (■) and PPARγ2 knockout (□) mice fed a normal diet (*A*) and an HFD (*B*). All wild-type values normalized to one for each gene ($n$ = 5–7). *$P$ < 0.05; **$P$ < 0.01.

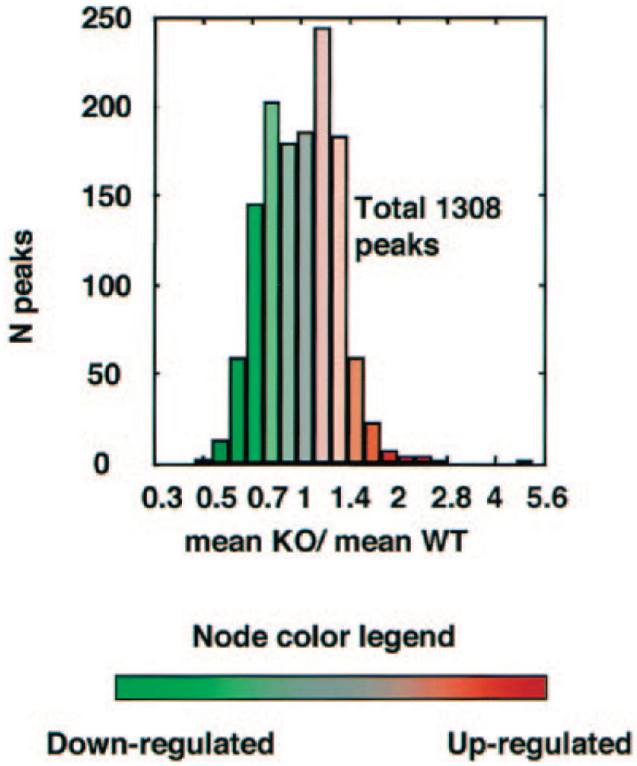


**FIG. 5.**

Lipidomic analyses in WAT of PPARγ2 knockout mice. Histogram showing the distribution of up-/downregulated processed peaks from LC/MS corresponding to lipid compounds. Height of each bar corresponds to number of peaks within a particular range of ratios of means (knockout [KO] vs. wild type [WT]).





Europe PMC Funders Author Manuscripts

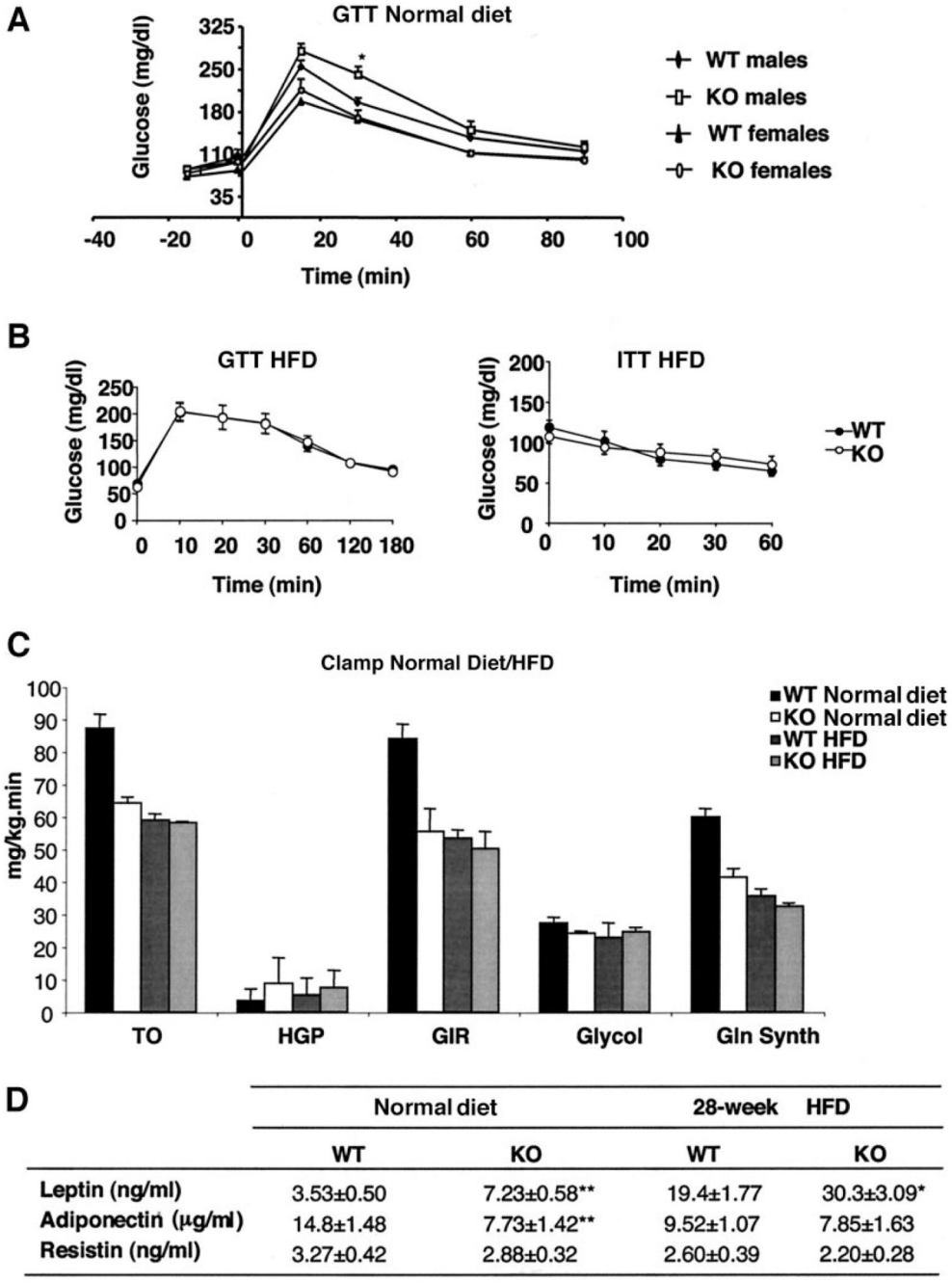


D

| | Normal diet | | 28-week HFD | |
|---|---|---|---|---|
| | WT | KO | WT | KO |
| Leptin (ng/ml) | 3.53±0.50 | 7.23±0.58** | 19.4±1.77 | 30.3±3.09* |
| Adiponectin (μg/ml) | 14.8±1.48 | 7.73±1.42** | 9.52±1.07 | 7.85±1.63 |
| Resistin (ng/ml) | 3.27±0.42 | 2.88±0.32 | 2.60±0.39 | 2.20±0.28 |

**FIG. 6.**

Effect of PPARγ2 deletion on insulin sensitivity. *A*: Plasma glucose levels during GTT in 16-week-old male and female mice fed a normal diet ($n = 7$). *$P < 0.05$ vs. wild type. *B*: Plasma glucose levels during GTT and ITT in male wild-type (•) and PPARγ2 knockout (○) mice fed 28 weeks of an HFD. *C*: Whole-body metabolic parameters during the euglycemic-hyperinsulinemic clamp experiment. Glucose turnover (TO), hepatic glucose production (HGP), glucose infusion rate (GIR), glycolysis (Glycol), and glycogen synthesis (Gln synth). Rates were obtained from male mice fed a normal diet (normal diet, $n = 7$) and an 28-week

HFD ($n$ = 6). *D*: Plasma adipokines levels from 32-week-old male wild-type and PPARγ2 knockout mice fed a normal diet and an HFD. KO, knockout; WT, wild type.



Europe PMC Funders Author Manuscripts

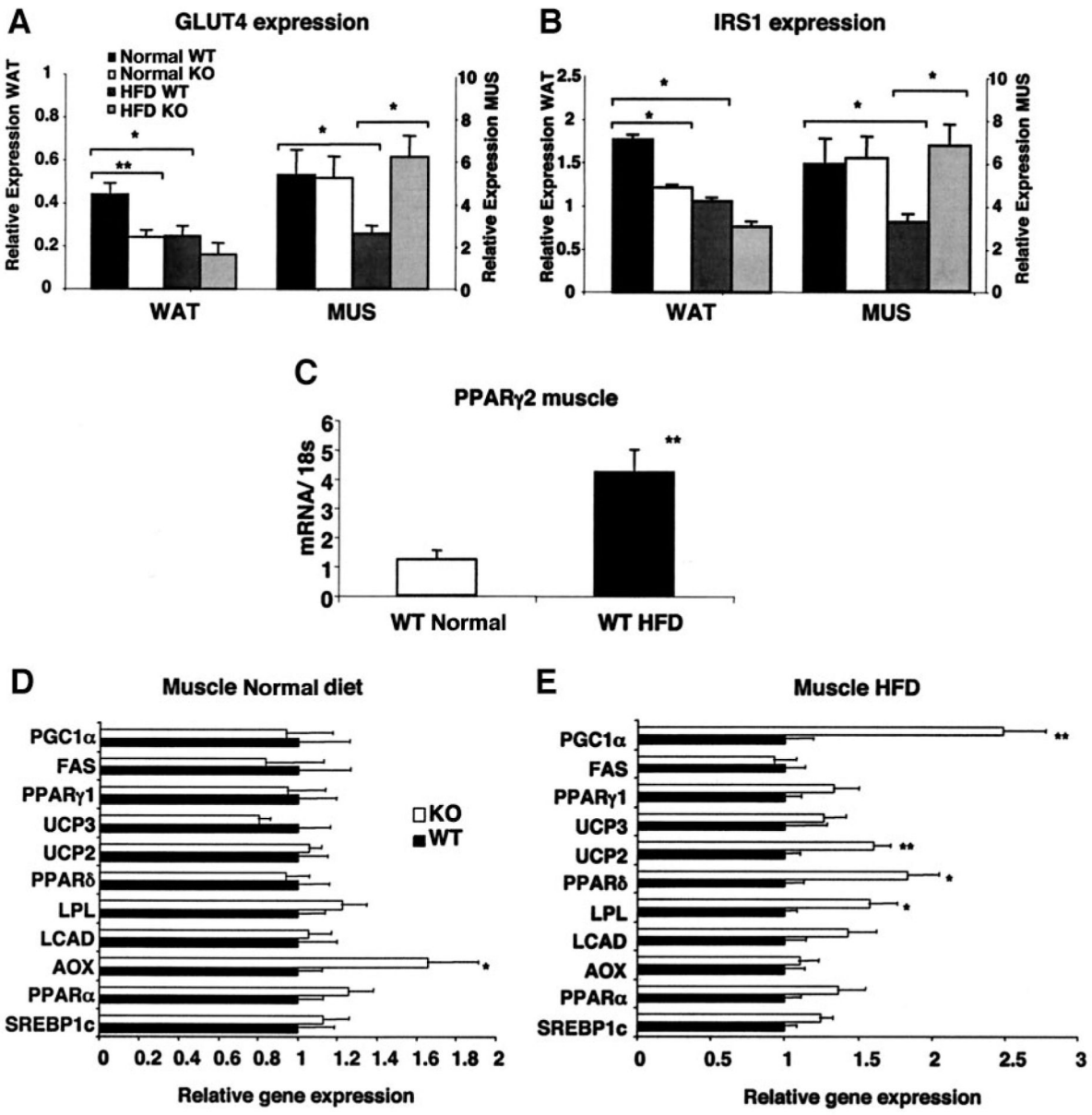


**FIG. 7.**

Gene expression analysis of PPARγ2-deficient skeletal muscle. Glut4 (*A*) and IRS-1 (*B*) mRNA levels in WAT and muscle from 16-week-old male wild-type (WT) and PPARγ2 knockout (KO) mice fed a normal diet and an HFD ($n = 5–8$). *C*: PPARγ2 mRNA levels in muscle of 16-week-old wild-type mice fed a normal diet and an HFD ($n = 5–7$). Skeletal muscle mRNA levels from different genes from 16-week-old male wild-type and PPARγ2 knockout mice fed a normal diet (*D*) and an HFD (*E*) ($n = 5–7$). *$P < 0.05$; **$P < 0.01$.




Europe PMC Funders Author Manuscripts

Europe PMC Funders Author Manuscripts

## TABLE 1

Metabolic parameters of 16-week-old male PPARγ2 knockout and wild-type mice

| | Normal diet | | 12 weeks on HFD | |
|---|---|---|---|---|
| | **Wild type** | **Knockout** | **Wild type** | **Knockout** |
| Glucose (mg/dl) | 130 ± 9.0 | 147 ± 5.9 | 236 ± 15.5 | 238 ± 11.1 |
| Glucose fasting (mg/dl) | 63 ± 4.1 | 88 ± 5.1† | 106.9 ± 12.8 | 113.0 ± 14.9 |
| Triglycerides (mmol/l) | 0.93 ± 0.12 | 0.87 ± 0.15 | 0.68 ± 0.17 | 0.78 ± 0.09 |
| Free fatty acids (μmol/l) | 295 ± 63 | 231 ± 17 | 250 ± 32 | 219 ± 22 |
| Insulin (μg/l) | 0.49 ± 0.10 | 0.34 ± 0.05 | 0.98 ± 0.20 | 1.31 ± 0.13 |
| Insulin fasting (μg/l) | 0.14 ± 0.03 | 0.35 ± 0.11 | | |
| Leptin (ng/ml) | 2.77 ± 0.44 | 4.13 ± 0.56* | 8.76 ± 1.13 | 16.66 ± 3.31* |
| Adiponectin (μg/ml) | 15.2 ± 1.2 | 7.9 ± 1.2‡ | 11.3 ± 1.09 | 7.46 ± 1.63* |

Data are means ± SE. $n$ = 5/10 for 16-week-old mice fed normal diet and HFD.

*$P < 0.05$

†$P < 0.01$

‡$P < 0.001$.